A Rocket-Triggered Lightning Flash Containing Negative-Positive-Negative Current Polarity Reversal during its Initial Stage

Fengquan Li [1, 2], Zhuling Sun [1]*, Rubin Jiang [1], Guoying Tang [3], Mingyuan Liu [1, 2], Xiao Li [1, 2], Hongbo Zhang [1], Shanfeng Yuan [1], Ye Tian [4], and Xiushu Qie [1, 2]

[1] Key Laboratory of Middle Atmosphere and Global Environment Observation, Institute of Atmospheric Physics, Chinese Academy of Sciences, Beijing 100029, China.

[2] College of Earth and Planetary Sciences, University of Chinese Academy of Sciences, Beijing 100049, China.

[3] Institute of Arid Meteorology, China Meteorological Administration, Lanzhou, 730020, China.

[4] Beijing Meteorological Observation Center, Beijing Meteorological Service, Beijing 100089, China.

Corresponding author: Zhuling Sun (sunzhuling@mail.iap.ac.cn)

Key Points:

- A rocket-triggered lightning flash with double current polarity reversals occurred under horizontal dipole charge structure.
- A reactivated breakdown bridged a negative leader and the grounding channel, rapidly reversing the current polarity to be positive.
- Recoil leaders injected negative charge to the grounding channel and caused positive current to decrease.

Abstract

A rocket-triggered lightning flash containing negative–positive–negative current polarity reversal during its initial stage is analyzed using multiple synchronized observation data. The flash was triggered under a thunderstorm transition zone between the convective region and the stratiform region. Both positive leaders developing in the transition zone and negative leaders developing toward the convective region could be identified. As the negative initial continuous current (ICC) declined, a negative leader was transformed from a recoil leader which turned to break down virgin air off the preconditioned positive leader branch. As the negative leader developing forward, a reactivated breakdown leader bridging the grounding trunk channel and the initiation region of the negative leader caused the current polarity reversed from negative to positive 0.22 ms later, which is reported for the first time. The negative leader channel terminated after propagating for 71.08 ms, and the ICC reversed to be negative again owing to the propagation of another positive branch. The horizontal dipole charge structure contributed to the branching of positive leader and the initiation of negative leader, which combined to produce the upward bipolar lightning. During the positive ICC stage, both positive and negative channels simultaneously contributed to the channel-base current and several negative recoil leaders injecting negative charge to the grounding trunk channel produced a fast decrease of the current.

1 Introduction

A bipolar lightning flash is one type of cloud-to-ground (CG) lightning flash that sequentially transfers charge of opposite polarity to ground. It can occur either in downward natural lightning (Saba et al., 2013; Saraiva et al., 2014; Tian et al., 2016), or upward lightning initiated from a high tower or windmill (Wang and Takagi, 2008; Zhou et al., 2011; Shi et al., 2018; Watanabe et al., 2019) or triggered lightning by a rocket-trailing-wire technique (Hubert and Mouget, 1981; Akiyama et al., 1985; Liu and Zhang, 1998; J Jerauld et al., 2004; Yoshida et al., 2012; Hill et al., 2013). Many previous studies have investigated the parameters (e.g., duration, peak current, and electric field change) of bipolar lightning (J Jerauld et al., 2004, 2009; Zhou et al., 2011; Nag and Rakov, 2012; Chen et al., 2015; Xue et al., 2015; Michishita et al., 2019) and classified bipolar lightning flashes into different types according to the stage that the current polarity reversal occurred in the flash (Rakov, 2003; Azadifar et al., 2016; Watanabe et al., 2019). However, the discharge processes and occurring mechanism of bipolar lightning are still not fully understood.

For natural CG bipolar lightning flashes, recoil leaders are found to be important in current polarity reversals. High-speed video imaging has revealed that recoil leaders retrace along a previous positive channel and produce a negative stroke after a positive stroke (Saba et al., 2013; Saraiva et al., 2014; Tian et al., 2016; Zhu et al., 2016). For an upward bipolar lightning initiated from a tower, Wang and Takagi (2008) observed that one branch of the positive leader decayed while another branch developed further. This changed the electric field at the tip of the decayed branch and thus a negative leader initiated and led to a current polarity reversal. Shi et al. (2018) further investigated this scenario using three bipolar lightning flashes based on lightning mapping array data and proposed that the cutoff on the trunk channel contributed to the current polarity reversal. In a triggered bipolar lightning flash, a negative leader inside the cloud was found to bridge the upper positive charge region and one branch of the upward positive leader, which led to a current polarity reversal (Yoshida et al., 2012). Mazur (2017) proposed that the downward positively charged branch of an intracloud flash initiated near the upward positive leader could intercept the cooling branch of the upward leader and cause a current polarity reversal. Besides in-cloud discharge processes causing the polarity reversal of the grounding channel, Azadifar et al. (2016) also reported that a bipolar lightning flash could be caused by sequential initiation of opposite-polarity upward leaders from a tower. Multiple branches of the upward leader successively propagating into opposite-polarity charge pockets might result in multiple current polarity reversals of a bipolar lightning flash in the initial continuous current (ICC) stage, but this still needs location evidence to confirm (Watanabe et al., 2019).

The occurrence of bipolar lightning flashes is closely related to the initiation and propagation processes of lightning, including the development of an intracloud leader, the discharges along opposite-polarity channels, and the maintenance and reversal of the current polarity of the channel. Although some observations have been made, the complicated mechanism of upward bipolar lightning is still unclear so far, and the above mentioned various current-reversal scenarios still need further investigation. Furthermore, investigating the occurrence of bipolar lightning would help to understand the initiation and propagation of lightning.

Two successively triggered lightning flashes with double current polarity reversals in the ICC stage were observed five minutes apart in the same thunderstorm. The first bipolar lightning flash with two return strokes is analyzed using multiple synchronized data in this study. The thunderstorm condition for the bipolar lightning flash is referred by using radar echo data. The initiation and development features of positive and negative leaders and the processes of the current polarity reversals are analyzed. This study will help to reveal how a complex cloud charge structure affects lightning initiation and propagation. The latter bipolar flash has been investigated by Tang et al. (2020) and will not be analyzed in detail here. To the best of our knowledge, the observation in this study is the first direct evidence to show that recoil leaders result in positive channel current to decrease and verify the phenomenon that lightning channels of opposite polarity can simultaneously affect the total current to ground.

2 Observation and data

A bipolar lightning flash was triggered using the classical rocket-and-wire technique in the SHAndong Triggering Lightning Experiment (SHATLE) at 15:47:36 UTC on 14 August 2015. The triggering site is in Zhanhua (37.82°N, 118.11°E), Shandong province, China, with the main observation site 970 m away (Wang et al., 2012; Jiang et al., 2013). Radar echo was from an S-band Doppler weather radar in Binzhou (37.35°N, 117.98°E), 53.41 km away from the triggering site. The surface electric field was measured with an electric field mill at the triggering site. Both 5 mΩ and 0.5 mΩ shunts with a bandwidth of 0 (direct current) ~3.2 MHz were applied to directly measure the channel-base current, and the upper limits for the measurable current were 2 kA and

40 kA, respectively. The minimum distinguishable current of the former shunt was about 9.3 A (Qie et al., 2017; Pu et al., 2019).

The lightning very-high-frequency (VHF) interferometer, fast antenna, and high-speed video camera were applied at the main site. Two-dimensional location results of lightning radiation sources with high time resolution, including azimuth and elevation, were obtained by the VHF interferometer and a detailed description can be found in (Sun et al., 2013, 2014). The bandwidth of the VHF interferometer was 140–300 MHz and the sampling rate was 1 GS s^{-1}. The VHF data recorded continuously for the duration of the flash. The time constant of the fast antenna was 0.1 ms with a bandwidth of 2 MHz. The sampling rate of the high-speed camera was 3200 fps, with an exposure time of 40 μs and a spatial resolution of 1280×800 pixels. Furthermore, multisite magnetic measurements were applied around the main site to provide the location of the low-frequency 3D lightning radiation sources. The magnetic measurement was conducted in a sampling rate of 1 MHz in a continuous mode. The baseline length ranged from 10-20 km and the bandwidth was 30-480 kHz. The location algorithm is similar to Lyu el al. (2014).

The data were synchronized with GPS time. All of the time-stamps used in this study are relative time, taking the instant when the upward positive leader initiated as the reference time. In practice, the instant when the pulse train occurred in current and electric field waveform was selected as the reference time. And as expected, elevation of the lightning VHF source location started to increase at this instant. Following the conventional definition in atmospheric electricity, the transfer of negative charge to ground corresponds to positive changes in the fast electric field change and currents with negative polarity.

3 Results

3.1 Thunderstorm condition of the triggered bipolar flash

A mesoscale convective system generated 160 km to the northwest of Zhanhua at about 04:55 UTC on 14 August 2015. The whole thunderstorm moved to the triggering site from the northwest to the southeast. The front convective edge of one cell associated with the triggered bipolar flash reached the triggering site at 14:02 and passed over at about 15:42. Then the trailing stratiform region was over the triggering site until the cell disappeared (Figure 1). The bipolar lightning flash was triggered at 15:47 when the triggering site was under the transition zone between the convective region and the stratiform region. The flash was initiated by the upward positive leader (UPL) and exhibited double current polarity reversals in its ICC stage.

Consistent with the development of the thunderstorm system, the surface electric field was small with some superimposed pulses before 15:00. After this, the surface electric field increased slowly to about 2–3 kV m^{-1} with some positive discharge processes, indicating that the dominant charge region that impacted the triggering site was of positive polarity. When the strong convective center moved away and the stratiform clouds approached the triggering site, the electric field slowly decreased to negative with infrequent lightning processes. The bipolar flash was triggered in this stage with a surface electric field of about −3.2 kV m^{-1}, when the dominant storm charge that impacted the triggering site was in negative polarity. About five minutes later, another bipolar lightning flash was triggered (Tang et al., 2020). After 16:20, electric field returned to positive (Figure 2).

The low-frequency 3D lightning location results for the bipolar flash in the plane view are superimposed on the composite radar reflectivity (Figure 1b) and the height-distance view is superimposed on the range-height indicator plot. After the initiation of the UPL, positive channels developed near the transition zone between the convective region and the stratiform region, with radar reflectivity ranging between about 30 and 40 dBZ. Two dart leaders inducing two return strokes sequentially in the bipolar flash initiated from the stratiform region with a radar reflectivity of about 25 dBZ in northeast of the triggering site.

The 3D results of the negative channels in the bipolar lightning flash from the low-frequency mapping are represented as dark gray dots in Figure 1b. The negative channels for the bipolar lightning flash propagated southwestward to the convective region with radar reflectivity ranging between about 40 and 50 dBZ. From Figure 1d, it can be seen that the positive and negative channels exhibited a horizontal distribution with the source height ranging from 2-5 km.

3.2 Overview of the bipolar lightning flash

Figure 1 shows the overview of the flash. The bipolar lightning flash lasted for about 480 ms. The whole process can be divided into three stages according to the current polarity, negative, positive, and negative. After the initiation of the UPL (at T0, 0 ms), the channel branched at an elevation of about 60°. Then many scattered channels developed forward. And some channels with dense and fast sources propagated toward the UPL, which were recoil leaders retrogressing back along previous positive leader channels. Three main positive branches labeled as PC1-3 in Figure 1 are recognized considering the initiation region and direction of recoil leaders. Near the end of the first negative current stage, a train of unipolar pulses superimposed on the fast electric change were detected, indicative of the negative stepped discharges in virgin air. The corresponding location sources are represented by the green colored dots and labeled as NC (negative channel) in Figure3 (and those dark gray dots in Figure 1). The NC initiated from positive branch PC3 and turned to break down virgin air continuously to the different direction of the positive leader. After NC initiation, the polarity of channel-base current changed to positive at T1 (221.87 ms). During the development of NC, many recoil leader-like processes occurred. The polarity of channel-base current changed from positive back to negative again at T2 (295.51 ms). Two dart leader-return stroke processes occurred later. Many recoil leader-like processes were detected during the whole flash, and eleven of them are presented here in detail and labeled as C1-C11, respectively. Animated lightning VHF sources for the whole flash can be found in the supplement（Movie S1).

Figure 4 shows the expanded variation of channel-base current, normalized fast electric field change, and lightning VHF source location map of the three stages with different polarity.

In stage 1 (~T0–T1, ~0–221.87 ms), the ICC was in negative polarity with a duration of about 221.87 ms, and a total of 19.95 C negative charge was transferred to ground. The UPL initiated at T0 and branched at high elevation with three main positive channels (PC1, PC2, and PC3) transferring negative charge to ground through the trunk channel. Two of the recoil leaders and subsequent breakdown processes on PC3 is marked as C1 and C2 in Figure 4a and b, respectively. At 210.42 ms, an NC initiated on the previous PC3 and broke down virgin air. The NC connected to the trunk channel and transferred positive charge to ground, resulting in the first current polarity reversal.

In stage 2 (~T1–T2, ~221.87–295.51 ms), a total of 8.64 C equivalent positive charge was transferred to ground. As the positive branches continued to progress with scattered positive discharges and frequent recoil leaders on channels, the NC propagated to low elevation. The NC did not touch ground as indicated by absence of return stroke in the fast electric field change waveform. Besides, the lightning mapping result from the magnetic field data also shows that the

NC propagated horizontally fay away from the site resulting in a reduction of the elevation (Figure 1 d). From 281.50 ms (71.08 ms after the initiation of the NC), no more lightning radiation sources were detected at the tip of the NC, indicating termination of the NC (Figure 4d).

Furthermore, seven recoil leaders sequentially initiated at almost the same position on the PC3 and then traced back along the PC3 channel. These recoil leaders then deviated the positive channel PC3 and formed stepped negative leaders, similar to the NC. Occurrence times for the seven recoil leaders are marked by C3–C9 in Figure 4c and their composite path is marked as C3-9 in Figure 4d, respectively. Unlike the NC, these negative leaders only lasted for several milliseconds. Among the seven recoil leader processes, the current had no obvious pulse during the development of C3, C8, and C9, while the current had a fast decrease during C4–C7 (especially C5 and C6).

At the end of stage 2, the channel-base current decreased continuously. The trunk channel remained luminous and the luminosity of the channel was relatively stable, as revealed by relative luminosity obtained from high-speed video images (See Figure S1 in Supplement). A typical initial continuous current pulse (ICCP) identified in the subsequent channel-base current waveform (Wang et al., 1999; Miki et al., 2005; Qie et al., 2014) indicated that the trunk channel was still active by discharges on positive branches around the end of stage 2. The moment when the channel-base current changed from positive to negative was determined as T2 (295.51 ms) by checking the nine-point moving average current waveform (inset in Figure 4c). The termination of the NC and the continued development of other positive branches combined to produce the second current polarity reversal.

In stage 3 (~T2–T3, ~295.51–480 ms), the lightning transferred negative charge of 8.15 C to ground. One ICCP and two dart leader-return strokes (DL-RS1 and DL-RS2) occurred. During the development of the two dart leaders DL1 and DL2, some radiation sources were detected to propagate from a branching point into the previous decayed positive branch (see Figure S2 in Supplement). The two return strokes shared the same channel and occurred about 45.01 ms apart. Furthermore, during stage 3, two recoil leaders C10 and C11 (similar to C3–C9 in stage 2) occurred on PC3, as shown by the blue location dots in Figure 4f.

3.3. In-depth look at the first current polarity reversal

At the end of stage 1, the ICC gradually decreased (Figure 5a). The positive channel PC1 had been decayed and scattered discharges were located on the PC2 (Figure 5b). Meanwhile, recoil leaders frequently occurred along the decayed positive channel PC3 towards the grounding trunk channel. Two recoil leader-like processes on PC3 are shown in Figure 5a and b, marked as C1 and C2, respectively. C1 initiated near point S1 at 202.5 ms and then propagated to higher elevation towards the direction of point S2 for 0.31 ms (the path of C1 is shown by blue dots and its direction is indicated by an arrow in Figure 5b). Considering that some previous recoil leaders were detected to propagate along the same path of C1, C1 should be a negative leader on PC3 propagating towards the trunk channel. C2 initiated at 203.25 ms near the tip of the decayed positive channel PC3 and retrograded along the PC3. Some breakdowns into virgin air during the development of C2 were detected. C2 stopped at point S3 after propagating for 10.43 ms. No current pulse associated with these recoil leaders was recorded, indicating that PC3 had been cut off from the trunk channel and negative charge was transferred to ground mainly by the active PC2.

During the progression of C2, the NC initiated from point S1 at 210.42 ms. The NC firstly propagated along the previous path of C1 (from point S1 to S2). About 0.27 ms later at 210.69 ms, the NC swerved near point S2 and then developed into virgin air. Positive pulses were superimposed on the electric field change showing that negative stepped leaders were propagating far away from the observation site. About 3.12 ms after the initiation of the NC, the C2 terminated at point S3 some distance away from the NC initiation region. The NC continued to progress with numerous branches and some scattered sources successively detected ahead of the tip of the positive leader PC3, showing that PC3 remained active with channel extension. PC3 and NC can be considered as the positive and negative parts of a bidirectional leader, respectively. And they formed a bipolar leader suspended from (or, not connected to) the trunk channel, and showed asymmetric development with a stronger negative leader part being NC.

The detailed discharges associated with the first current polarity reversal (at T1, 221.87 ms) are shown in Figure 5c and d. After the NC had propagated forward for 11.23 ms, a reactivated breakdown leader initiated at about 221.65 ms from the point S4 and developed towards the initiation region of the NC (Figure 5c and d), and the corresponding current was relatively stable. About 80 μs later at 221.73 ms, a positive pulse in the fast electric field change was detected with a sudden burst of relative VHF radiation power (shaded region in Figure 5c and e), and corresponding VHF lightning sources were located near the initiation region of the NC (Figure 5d and f). This means that the reactivated breakdown leader contacted the floating bidirectional leader of PC3 and NC (Stock et al. 2017; Pu and Cummer, 2019). A VHF location source occurring nearest to the instant of the positive electric pulse was selected as the contact point S5 (Figure 5f). The channel-base current rapidly reduced to zero in 0.14 ms (at T1, 221.87 ms, namely, 0.22 ms after the initiation of the reactivated breakdown) and continued to positively increase, as positive charge of the floating bipolar leader had been transported along the trunk channel to ground. The later part of the path of the reactivated breakdown leader and the initiation path of NC had some overlaps (Figure 5f). The reactivated breakdown effectively bridged the grounding trunk channel and the initiation region of the NC.

3.4 Recoil leaders caused the positive current to decrease

After the first current polarity reversal, seven recoil leader-like processes occurred on PC3 in stage 2, but some of them (C3, C8, and C9) did not produce obvious pulse in the current waveform, while others (C4–C7) caused fast decreases of the channel-base current. The processes of C6 are presented because few discharge processes occurred on other positive channels before or during the development of C6. In this situation, we can determine that the decrease of positive current was caused by C6.

As can be seen in Figure 6a and b, before the initiation of C6 (at 271.76 ms), the positive channel-base current was decreasing and the electric field change seemed flat, although the NC still developed towards lower elevation. An abrupt decrease of the electric field change occurred after C6 initiated from the tip of the previous positive channel PC3 and progressed back along PC3. About 0.48 ms after its initiation (at 272.24 ms), C6 reached point S3 and deviated from the previous path of PC3 at point S3. The point S3 here was also the location where C2 terminated (S3 in Figure 5). Then it turned into the path previously ionized by C4-5 and propagated towards lower elevation as indicated by the arrow, and finally transformed into a relatively slow negative breakdown in the virgin air towards two directions. The trend of the electric field change waveform varied due to the forward direction of C6 swerving relative to the main observation site. During the sharp negative change of the electric field, the current started a fast decrease of about 0.04 kA (0.11 ms after the C6 reached point S3, at 272.35 ms). And then it had a small increase. This behavior is similar to M process (Shao et al. 1995) but it was superimposed on a positive background current. The peak of the current lagged behind the electric field peak by about 170 μs. Then the electric field and current gradually increased and became relatively stable. The C4–C7 showed the same propagation behavior and a similar current decrease. It shows that negative charge was injected into the grounding channel by these recoil leaders and reduced the positive channel-base current.

Before the end of stage 2, the NC terminated and no more positive current was transferred to ground. Termination of the NC and the occurrence of these recoil leaders combined to contribute to the second current polarity reversal.

4 Discussion

A triggered lightning flash exhibiting negative-positive-negative polarity shift in its ICC stage is analyzed. One branch (PC3) of the upward positive leader was cut off to trunk channel. Recoil leaders successively occurred on the decayed positive channel PC3. One of the recoil leaders deviated from PC3 and turned to break down the virgin air. It finally formed a negative channel NC. A reactivated breakdown bridged the grounding trunk channel and the initiation region of the NC. This process caused current rapidly reverse from negative to positive. In this section, we will discuss how the horizontal dipole storm charge distribution affects the current polarity reversal. The fast decreases of positive ICC caused by negative recoil leaders will also be discussed.

4.1. Current polarity reversal due to storm charge configuration

In the case of this study, the propagating direction of the positive channels PC1-3 was northeast and the propagating direction of NC was southwest. This phenomenon that different-polarity channels propagated in opposite directions is also found in the triggered bipolar lightning in Tang et al. (2020). Horizontally separated distribution of the positive and negative charge regions might contribute to the occurrence of this bipolar lightning.

Figure 7 shows a schematic of the first and second current polarity reversals based on the lightning mapping results. In a rocket-triggered lightning or an upward lightning initiated from a high tower or windmill, the UPL splits into two branches that develop simultaneously in the cloud, like branch 1 and branch 2 in Figure 7a. The current of branch 1 could be cutoff from the trunk channel at some point, possibly owing to the influence of a strong positive charge region nearby and the uneven development of positive branches or the screening effect (Mazur and Ruhnke, 2014) (Figure 7b). Meanwhile, the conductive branch 2 keeps propagating forward and transferring negative charge back to the trunk channel. The channel near the cutoff point will be cooling and losing electrical conductivity (Williams and Heckman, 2012). The potential would be much closer to the local potential for the tip of the low-current branches which spilt from the original positive leader (van der Velde and Montanyà, 2013). This would cause electric field near the cutoff point to increase. As a consequence, a bidirectional recoil leader will occur and its negative end would trace back along the previous branch 1 when the electric field is high enough (Figure 7c). In some situations, such as when there is a large positive charge region nearby, the ambient electric potential near point B will become stronger than that ahead of the recoil leader and the recoil leader will turn into a slow negative leader breaking down virgin air from the point B (Figure 7d). After the initiation of the negative leader, it would develop in a bidirectional way with the positive end being Branch 1. As the negative leader progresses towards the direction with high potential, the potential of the floating bidirectional channel increases. When the electric field between the floating channel and the grounding trunk channel reverses and becomes higher than breakdown threshold, a reactivated bipolar leader will occur on the previous cutoff channel with the negative end developing towards the floating channel and the positive end towards the grounding trunk channel. The reactivated leader effectively bridged the grounding trunk channel and the negative leader NC. The NC thus will connect to the trunk channel and transfer positive charge to ground through the bridge (Figure 7e). The polarity of net charge transferred to ground will shift from negative to positive if the negative channel dominates the discharge process, producing the first current polarity reversal. The negative leader will terminate when the electric field is not high enough to maintain its propagation (Mazur and Ruhnke, 2014). No more positive charge will be transferred to the grounding trunk channel while the other positive channels keep transferring negative charge to ground. Thus, the second current polarity reversal occurs (Figure 7f).

The phenomenon of a negative leader initiating on a positive channel as shown in Figure 7d was also reported in natural lightning. Pu and Cummer (2019) found that a nearby active positive leader induced the initiation of negative leaders from the inner negative charge layer in the previous positive channel. Saraiva et al. (2014) found that cutoff occurred on the positive branch and a recoil leader retraced back and then deviated from the previous positive branch, thus initiating a negative leader. The phenomenon that recoil leaders retraced back along previous channel and then turned to break down virgin air has also been reported in Stolzenburg et al. (2020). The variation of electric field was also considered to be major factors for current polarity reversals in the studies of upward bipolar lightning. Hill et al. (2013) reported a negative leader initiated from the horizontal positive leader and propagated towards the upper positive charge region, leading to a current polarity reversal in a triggered bipolar lightning flash. In their study, the initiation of the upward negative leader was inferred to be linked to spatial variation of ambient electric field. Wang and Takagi (2008) and Shi et al. (2018) found a negative leader initiated at the tip of a decayed positive branch because the electric field along the decayed positive branch reversed in direction. For the case in this study, the NC firstly initiated at the location where C1 initiated and then propagated along the path of C1 for some distance and finally deviated from the positive channel PC3 and turned to break down virgin air (as shown in Figure 5b). Before C1, there has been some recoil leaders that travelled along the same path of C1. Therefore, the scenario of NC initiation in this study is unlike that in Shi et al. (2018) in which the negative channel directly initiated at the tip of the previous positive branch. However, it is reasonable to infer that the NC deviated from the main channel PC3 and then travelled along some small branches near point S2 as shown in Figure 5b (corresponding to point B in Figure 7) and finally broke down virgin air from the tip of these branches. Another possible scenario of NC initiation in this study is that the NC directly initiated on the PC3 firstly as a needle like that in Pu and Cummer (2019) and then developed continuously in the virgin air. In this study, many channels overlapped near the NC initiation location on the two-dimensional lightning VHF location map due to the clustered discharge processes. This brings some difficulties for a more detailed analysis.

Besides the negative channel NC which was related to the current polarity reversal, C4–11 were also found to first retrace back along the previous positive branch and then deviated, producing new negative stepped leaders. Unlike the NC, these negative leaders C4-11only lasted for several milliseconds. In addition, during the development of the two dart leaders, some radiation sources were detected to propagate from a branching point into a previous decayed positive branch (as shown in Figure S2). This indicates that the electric field along the previous branch indeed reversed. These breakdowns did not develop further or produce a negative leader, unlike Shi et al. (2018), probably because the ambient electric field was not strong enough to either support the initiation of a negative leader or maintain its development. Under appropriate conditions, it is possible that a new negative leader could be generated either by a recoil leader deviating from the previously ionized positive channel or by electric field reversal at the tip of the small decayed positive branch.

Hill et al. (2013) and Shi et al. (2018) reported other cases of a separated distribution of charge regions, which also resulted in the occurrence of an upward triggered bipolar lightning. In their studies, charge regions were vertically distributed with a positive charge region above the negative charge region. In this study, the horizontally separated distribution of the positive and negative charge regions influenced the development of lightning channels, especially the negative channel, and caused the two current polarity reversals. We infer that no matter in which form the opposite-polarity charge regions are separated (vertical, horizontal, or tilted), if the lightning discharge channels are located near the interface of positive and negative charge regions, the leaders might propagate into opposite-polarity charge regions and successively transfer opposite-polarity charge to ground.

4.2. Opposite-polarity channel simultaneously contributes to the total current to ground

For CG lightning, the grounding trunk channel bridges the in-cloud charge region and ground as a current transmission path. Actually, the in-cloud channels connecting the grounding channel can affect the channel current. Usually, when a recoil leader retracing back along the decayed positive channel connected to the grounding channel, it will cause an increase of negative channel-base current, such as M process (Shao et al. 1995). In this flash case, during the positive ICC stage, the dominated intra-cloud charge was negative, and some recoil leaders (such as C6 in Figure 6) were detected to trace back along the decayed positive leader and caused the positive current to decrease. Furthermore, after the NC ceased to develop (at the end of the positive ICC stage), the channel-based current transformed from positive to negative gradually and after that a recoil leader that connected to the trunk channel produced an ICCP (as shown in Figure 4c and d). On this basis, it is inferred that opposite-polarity channel (corresponding to the Branch 1 and the negative leader shown in Figure 7d) simultaneously contributes to the total current to ground during the positive ICC stage. The negative channel transferred positive charge to the trunk channel while the positive channel intermittently injected negative charge to the trunk channel by producing recoil leaders or positive breakdowns. Similarly, Yoshida et al. (2012) reported one negative branch of an intracloud discharge connected to one positive branch of the UPL in a bipolar triggered lightning flash. Hill et al. (2013) proposed that both positive and negative charge sources might be simultaneously available to the channel to ground for negative ICCP-like pulses during the positive ICC stage. However, intracloud discharges leading to those pulses were not discussed in their studies owing to the lack of a detailed description of the branches and the relatively low time resolution of the location results from lightning mapping array data. Besides, in their studies, the reconnection processes were not deeply investigated. In this study, a reactivated breakdown leader was detected to cause the negative channel connecting to the grounding trunk channel. The reactivated breakdown leader might be a bidirectional leader as shown in Figure 7e. However, only a negative leader with strong VHF power was mapped by VHF lightning location system in this flash case. The reason may be that the VHF emission of the breakdowns on positive end was weaker and thus masked by the negative end (Shao et al., 1995, 1999; Edens et al., 2012).

5 Conclusion

A rocket-triggered lightning flashes containing negative–positive–negative current polarity reversal during its initial stage of the continuing current is analyzed using comprehensive data, including channel-based current, two-dimensional radiation mapping from a VHF lightning interferometer, fast electric field change, and high-speed video images. With the multiple-source data, in particular, the VHF lightning interferometer mapping, the detailed discharge processes are investigated and a physical mechanism for the double current polarity reversals is proposed. Conclusions are drawn as follows.

As the thunderstorm passed over the triggering site, a bipolar lightning flash was triggered under the transition zone between the convective region and the stratiform region with radar reflectivity of 30-40 dBz. The dominant charge region that impacted the triggering site was of negative polarity. During the ICC stage, positive leaders developed in the transition zone and negative leaders developed horizontally toward the convective region. During the reduction of the first negative initial current, a recoil leader retrograded along one decayed positive branch and deviated from the previous path as a new negative leader breaking down the virgin air. The decayed positive branch became reactive and formed a bidirectional channel with the negative leader. About 11.23 ms after the negative leader initiation, as a reactivated breakdown occurred between the grounding trunk channel and the initiation region of the negative leader, the floating bidirectional channel reconnected to the trunk channel and resulted in the current reversing rapidly to be positive 0.22 ms later. The connection to the trunk channel happened somewhere in between the two floating leader tips. During the positive ICC stage, recoil leaders occasionally occurred on the positive part of the bidirectional channel, and injected negative charge to the grounding trunk channel, producing fast decrease of positive current. The time duration of the negative leader was 71.08 ms. The ICC reversed to be negative again with the termination of negative leader and the propagation of another positive branch.

The horizontal dipole charge distribution contributed to the branching structure of positive leader and the initiation of negative leader, which combined to result in the upward bipolar lightning flash. The phenomenon that opposite-polarity channel simultaneously contributed to the total current to ground is verified for the first time in this study. This phenomenon might have occurred in the previous studied cases, but information of the propagation of different channels was not effectively captured. Some details of the discharge process still could not be determined in this study, as some channels were overlapping in the 2D lightning map from the single-station VHF interferometer, and the time resolution of the 3D lightning location results provided by the magnetic measurements was low. In future, it is necessary to utilize high-resolution 3D lightning location mapping and electric field sounding to further verify the proposed mechanism of current polarity reversal.

Acknowledgments

The research was supported by National Natural Science Foundation of China (grants 41875008, 41775012, and 41630425); Key Research Program of Frontier Sciences, CAS (grant QYZDJ-SSW-DQC007); and National Key Research and Development Program of China (grant No. 2017YFC1501502). The authors thank Yunjiao Pu for her valuable comments. This work complies with the AGU data policy. Refer to the data repository website (https://zenodo.org/record/4052245) for data availability.

References

Akiyama, H., Ichino K. & Horii K. (1985), Channel reconstruction of triggered lightning flashes with bipolar currents from thunder measurements, J. Geophys. Res. Atmos., 90(D6), 10674-10680, doi:10.1029/JD090iD06p10674.

Azadifar, M., Rachidi F., Rubinstein M., Rakov V. A., Paolone M., & Pavanello D. (2016), Bipolar lightning flashes observed at the Säntis Tower: Do we need to modify the traditional classification?, J. Geophys. Res. Atmos., 121(23), 14,117-114,126, doi:10.1002/2016jd025461.

Chen, L., Lu W., Zhang Y., & Wang D. (2015), Optical progression characteristics of an interesting natural downward bipolar lightning flash, J. Geophys. Res. Atmos., 120(2), 708-715, doi:10.1002/2014jd022463.

Edens, H. E., Eack K. B., Eastvedt E. M., Trueblood J. J., Winn W. P., Krehbiel P. R., et al. (2012). VHF lightning mapping observations of a triggered lightning flash. Geophys. Res. Lett., 39(19). doi:10.1029/2012gl053666

Hill, J. D., Pilkey, J., Uman, M. A., Jordan, D. M., Rison, W., Krebhiel, P. R., et al. (2013), Correlated lightning mapping array and radar observations of the initial stages of three sequentially triggered Florida lightning discharges, J. Geophys. Res. Atmos., 118, 8460– 8481, doi:10.1002/jgrd.50660.

Hubert, P., & Mouget G. (1981), Return stroke velocity measurements in two triggered lightning flashes, J. Geophys. Res., 86(C6), doi:10.1029/JC086iC06p05253.

Jerauld, J. E., Uman M. A., Rakov V. A., Rambo K. J., & Jordan D. M. (2004), A triggered lightning flash containing both negative and positive strokes, Geophys. Res. Lett. 31(8), doi:10.1029/2004GL019457.

Jerauld, J. E., Uman M. A., Rakov V. A., Rambo K. J., Jordan D. M., & Schnetzer G. H. (2009), Measured electric and magnetic fields from an unusual cloud-to-ground lightning flash containing two positive strokes followed by four negative strokes, J. Geophys. Res., 114(D19), doi:10.1029/2008jd011660.

Jiang, R., Qie X., Yang J., Wang C., & Zhao Y. (2013), Characteristics of M-component in rocket-triggered lightning and a discussion on its mechanism, Radio Sci., 48, 597–606, doi: 10.1002/rds.20065.

Liu, X., & Zhang Y. (1998), Review of artificially triggered lightning study in China, IEEJ Transactions on Power and Energy, 118(2), 170-175, doi:10.1541/ieejpes1990.118.2_170.

Lyu, F., Cummer S. A., Solanki R., Weinert J., McTague L., Katko A., et al. (2014), A low-frequency near-field interferometric-TOA 3-D Lightning Mapping Array, Geophys. Res. Lett., 41, 7777–7784, doi:10.1002/2014GL061963.

Mazur, V. (2017), On the nature of bipolar flashes that share the same channel to ground, Journal of Electrostatics, 90, 31-37, doi:10.1016/j.elstat.2017.09.002.

Mazur, V., & Ruhnke L. H. (2014), The physical processes of current cutoff in lightning leaders, J. Geophys. Res. Atmos., 119(6), 2796-2810, doi:10.1002/2013jd020494.

Michishita, K., Yokoyama S., & Honjo N. (2019), Measurement of lightning current at wind turbine near coast of Sea of Japan in winter, IEEE Transactions on Electromagnetic Compatibility., doi: 10.1109/TEMC.2019.2913195.

Miki, M., Rakov V. A., Shindo T., Diendorfer G., Mair M., Heidler F., et al. (2005), Initial stage in lightning initiated from tall objects and in rocket‐triggered lightning, J. Geophys. Res. Atmos., 110(D2), doi: doi:10.1029/2003JD004474

Nag, A., & Rakov, V. A. (2012), Positive lightning: An overview, new observations, and inferences, J. Geophys. Res., 117, D08109, doi:10.1029/2012JD017545.

Pu, Y., & Cummer S. A. (2019), Needles and Lightning Leader Dynamics Imaged with 100–200 MHz Broadband VHF Interferometry, Geophys. Res. Lett., 46(22), 13556-13563, doi:10.1029/2019gl085635.

Pu, Y., Qie X., Jiang R., Sun Z., Liu M., & Zhang H. (2019). Broadband characteristics of chaotic pulse trains associated with sequential dart leaders in a rocket‐triggered lightning flash. J. Geophys. Res. Atmos., 124, 4074–4085. doi:10.1029/2018JD029488

Qie, X., Jiang R., & Yang J. (2014), Characteristics of current pulses in rocket-triggered lightning, Atmos. Res., 135, 322-329. doi: 10.1016/j.atmosres.2012.11.012.

Qie X., Pu Y., Jiang R., Sun Z., Liu M., Zhang H., et al., (2017), Bidirectional leader development in a preexisting channel as observed in rocket-triggered lightning flashes. J. Geophys. Res. Atmos., 122: 586–599, doi:10.1002/2016JD025224

Rakov, V. A. (2003), A Review of Positive and Bipolar Lightning Discharges, Bulletin of the American Meteorological Society, 84(6), 767-776, doi:10.1175/bams-84-6-767.

Saba, M. M. F., Schumann C., Warner T. A., Helsdon J. H., Schulz W., & Orville R. E. (2013), Bipolar cloud-to-ground lightning flash observations, J. Geophys. Res. Atmos., 118(19), 11,098-011,106, doi:10.1002/jgrd.50804.

Saraiva, A., Campos L., Williams E., Zepka G., Alves J., Pinto Jr O., et al. (2014), High‐speed video and electromagnetic analysis of two natural bipolar cloud‐to‐ground lightning flashes, J. Geophys. Res. Atmos., 119(10), 6105-6127, doi:10.1002/2013jd020974.

Shao, X. M., Krehbiel, P. R., Thomas, R. J., & Rison, W. (1995). Radio interferometric observations of cloud-to-ground lightning phenomena in Florida. J. Geophys. Res. Atmos., 100(D2), 2749-2783. doi:10.1029/94jd01943

Shao, X. M., Rhodes, C. T., & Holden, D. N. (1999). RF radiation observations of positive cloud-to-ground flashes. J. Geophys. Res. Atmos., 104(D8), 9601-9608. doi:10.1029/1999jd900036

Shi, D., Wang D., Wu T., Thomas R. J., Edens H. E., Rison W., et al. (2018), Leader polarity-reversal feature and charge structure of three upward bipolar lightning flashes, J. Geophys. Res. Atmos., 123(17), 9430-9442, doi:10.1029/2018jd028637.

Stock, M. G., Krehbiel P. R., Lapierre J., Wu T., Stanley M. A., & Edens H. E. (2017), Fast positive breakdown in lightning, J. Geophys. Res. Atmos., 122, 8135–8152, doi:10.1002/2016JD025909

Stolzenburg, M., Marshall, T.C. & Karunarathne, S. (2020), Inception of subsequent stepped leaders in negative cloud-to-ground lightning. Meteorol Atmos Phys 132, 489–514. doi:10.1007/s00703-019-00702-8

Sun, Z., Qie X., Liu M., Cao D., & Wang D. (2013), Lightning VHF radiation location system based on short-baseline TDOA technique—validation in rocket-triggered lightning, Atmos. Res. 129-130: 58–66. doi: 10.1016/j.atmosres.2012.11.010

Sun, Z., Qie, X., Jiang, R., Liu, M., Wu, X., Wang, Z., et al. (2014), Characteristics of a rocket‐triggered lightning flash with large stroke number and the associated leader propagation, J. Geophys. Res. Atmos., 119, 13,388– 13,399, doi:10.1002/2014JD022100.

Tang, G., Sun Z., Jiang R., Li F., Liu M., Liu K., & Qie X. (2020), Characteristics and mechanism of a triggered lightning with two polarity reversals of charges transferred to ground, Acta Phys. Sin., doi:10.7498/aps.69.20200374

Tian, Y., Qie X., Lu G., Jiang R., Wang Z., Zhang H., et al. (2016), Characteristics of a bipolar cloud-to-ground lightning flash containing a positive stroke followed by three negative strokes, Atmos. Res., 176-177, 222-230, doi:10.1016/j.atmosres.2016.02.023.

van der Velde, O. A., & Montanyà J. (2013), Asymmetries in bidirectional leader development of lightning flashes, J. Geophys. Res. Atmos., 118, 13,504–13,519, doi:10.1002/2013JD020257.

Wang C., Qie X., Jiang R. & Yang J. (2012). Propagating properties of a upward positive leader in a negative triggered lightning, Acta Phys. Sin., 61(3): 039203. doi: 10.7498/aps.61.039203

Wang, D., & Takagi N. (2008), Characteristics of upward bipolar lightning derived from simultaneous recording of electric current and electric field change, Proc. of URSI E, 6, 2.

Wang, D., Rakov V. A., Uman M. A., Fernandez M. I., Rambo K. J., Schnetzer G. H., & Fisher R. J. (1999), Characterization of the initial stage of negative rocket-triggered lightning, J. Geophys. Res. Atmos., 104(D4), 4213-4222. doi: 10.1029/1998JD200087

Watanabe, N., Nag A., Diendorfer G., Pichler H., Schulz W., Rakov V. A., & Rassoul H. K. (2019), Characteristics of currents in upward lightning flashes initiated from the gaisberg tower, IEEE Transactions on Electromagnetic Compatibility, 1-14, doi:10.1109/temc.2019.2916047.

Williams, E., & Heckman S. (2012), Polarity asymmetry in lightning leaders: The evolution of ideas on lightning behavior from strikes to aircraft.

Xue, S., Yuan P., Cen J., Li Y., & Wang X. (2015), Spectral observations of a natural bipolar cloud-to-ground lightning, J. Geophys. Res. Atmos., 120(5), 1972-1979, doi:10.1002/2014jd022598.

Yoshida, S., Biagi C., Rakov V. A., Hill J., Stapleton M., Jordan D., et al. (2012), The initial stage processes of rocket‐and‐wire triggered lightning as observed by VHF interferometry, J. Geophys. Res. Atmos., 117(D9), doi:10.1029/2012jd017657.

Zhou, H., Diendorfer G., Thottappillil R., Pichler H., & Mair M. (2011), Characteristics of upward bipolar lightning flashes observed at the Gaisberg Tower, J. Geophys. Res. Atmos., 116(D13), doi:10.1029/2011jd015634.

Zhu, Y., Rakov V. A., Tran M. D., & Lu W. (2016), A subsequent positive stroke developing in the channel of preceding negative stroke and containing bipolar continuing current, Geophys. Res. Lett., 43(18), 9948-9955, doi:10.1002/2016gl070475.

Figure 1. Radar reflectivity and low-frequency 3D lightning location results of the bipolar lightning flash. (a-c): Composite radar reflectivity from 15:42 to 15:54 UTC on 14 August 2015 at 6-min interval, and low-frequency 3D lightning location results in the plane view are superimposed on the radar echo in (b). (d): range-height indicator from point A to point B at 15:48 UTC with height-distance view of low-frequency 3D lightning sources superimposed. Light gray dots represent positive channels (including the dart leaders and return strokes) and the dark gray dots represent negative channels. The triggering site is indicated by the black plus.

Figure 2. Variation of surface electric field during the thunderstorm. Triggering times of the bipolar lightning flashes in this study and Tang et al. (2020) are marked by red arrows.

Figure 3. Observation results for the overall bipolar triggered lightning flash. Channel-base current, normalized squared VHF power and electric field change (a), lightning VHF source elevation (b), and overview of the lightning VHF source location 2D mapping (c). ICCP represents the initial continuous current pulse, and DL-RS represents the two dart leader- return strokes.

Black inverted triangles on the top mark the times of initiation of UPL (at T0, 0 ms), the current polarity reversals (at T1, 221.87 ms and at T2, 295.51 ms), and the end of the lightning (at T3, 480 ms). In (b) and (c), UPL (light gray) represent upward positive leader, PC1, PC2, and PC3 (pink) represent positive channels, NC (green) represents negative channel, C1 and C2-11 (blue) represent recoil leaders and some subsequent process, and DL-RS (dark gray) represents the sources of two dart leader–return stroke processes. The positive channel PC2 was reconstructed by overlaying the path of two dart leaders and return strokes. The position of the rocket launcher and trunk channel are also marked in (c).

Figure 4. Observation results for the bipolar lightning flash during different stages. Expanded variation of channel-base current and normalized electric field change (a, c, and e), and lightning VHF source location (b, d, and f) in stage 1 (a and b), stage 2 (c and d), and stage 3 (e and f). Dark gray dots in superimposed in (b, d, and f) depict the path of two dart leader–return strokes that occurred in stage 3. Light gray dots represent the composite lightning source location before T1 (221.87 ms) and T2 (295.51 ms) for (e) and (f), respectively. The inset in (c) shows the nine-point running mean of channel-base current near the end of stage 2.

Figure 5. In-depth look at the observation results near the first current polarity reversal (at T1, 221.87 ms). Variation of channel-base current and normalized electric field change (a and c, with elevation of lightning sources superimposed in c), VHF source location map (b and d), and relative VHF power (e) before and after the first current polarity reversal; expanded view of VHF location map for the reactivated breakdown leader (color shows the time variation)with the previous process of NC initiation (clustered with light gray dots) overlaid (f). Shaded region in (a) marks the duration of C2. The inset in (b) shows the expanded view of the NC that initiated and developed along the previous recoil leader C1. The region shown in Panel (d) corresponds to the region marked with a box in panel (b); the region shown in Panel (f) is an expanded view of panel (d) but the light gray dots only consists of the lightning sources of NC initiation. In panel (b) and (d), dark gray dots depict the path of dart leader–return strokes that occurred in stage 3 while light gray dots depict the lightning sources occurred previously. The shaded region in (c) and (e) marks the time

range when a positive pulse in the fast electric field change and a sudden burst of relative VHF radiation power occurred. The time for the data in (a) and (b) ranged from 201.00 ms to 222.70 ms and the lightning sources are coded with color consistent with Figure 3 and 4. While the time for the data in (c) to (f) ranged from 221.60 ms to 221.90 ms and colors (from blue to red) represent the variation of time. Different marker shapes in panel c-f differentiate the lightning source location of PC3 (triangles), NC (squares) and the reactivated breakdown (circles).

Figure 6. Observation results near the recoil leader C6 in stage 2. Variation of channel-base current and normalized electric field change (a), lightning VHF source location map (b) for C6. Colored dots in (b) represent paths (color from blue to red represents the variation of time). Point S6 in (b) represents the location of the initiation point of C6. Point S3 represents the location where C6 connected to the trunk channel and deviated from PC3. Note that the point S3 in panel b is the same with the point S3 in Figure 5.

Figure 7. Schematic of the mechanism of double current polarity reversals. (a) UPL with two positive branches. (b) A cutoff occurred on branch 1while branch 2 continued to develop and positive breakdown at its tip transferred negative charge back, (c) a recoil leader occurred on branch 1, (d) negative charge accumulated near point B, and then a negative channel initiated at point B and formed a floating bidirectional leader with branch 1. (e) The tip of the negative leader developed and transferred positive charge back to its tail end B. A reactivated breakdown leader occurred from the trunk channel to the floating channel, thus the negative leader connected to the trunk channel and the current polarity reversed. (f) The negative leader decayed while the positive branches remained, producing the second current polarity reversal. The plus and minus signs represent the polarity of charge.

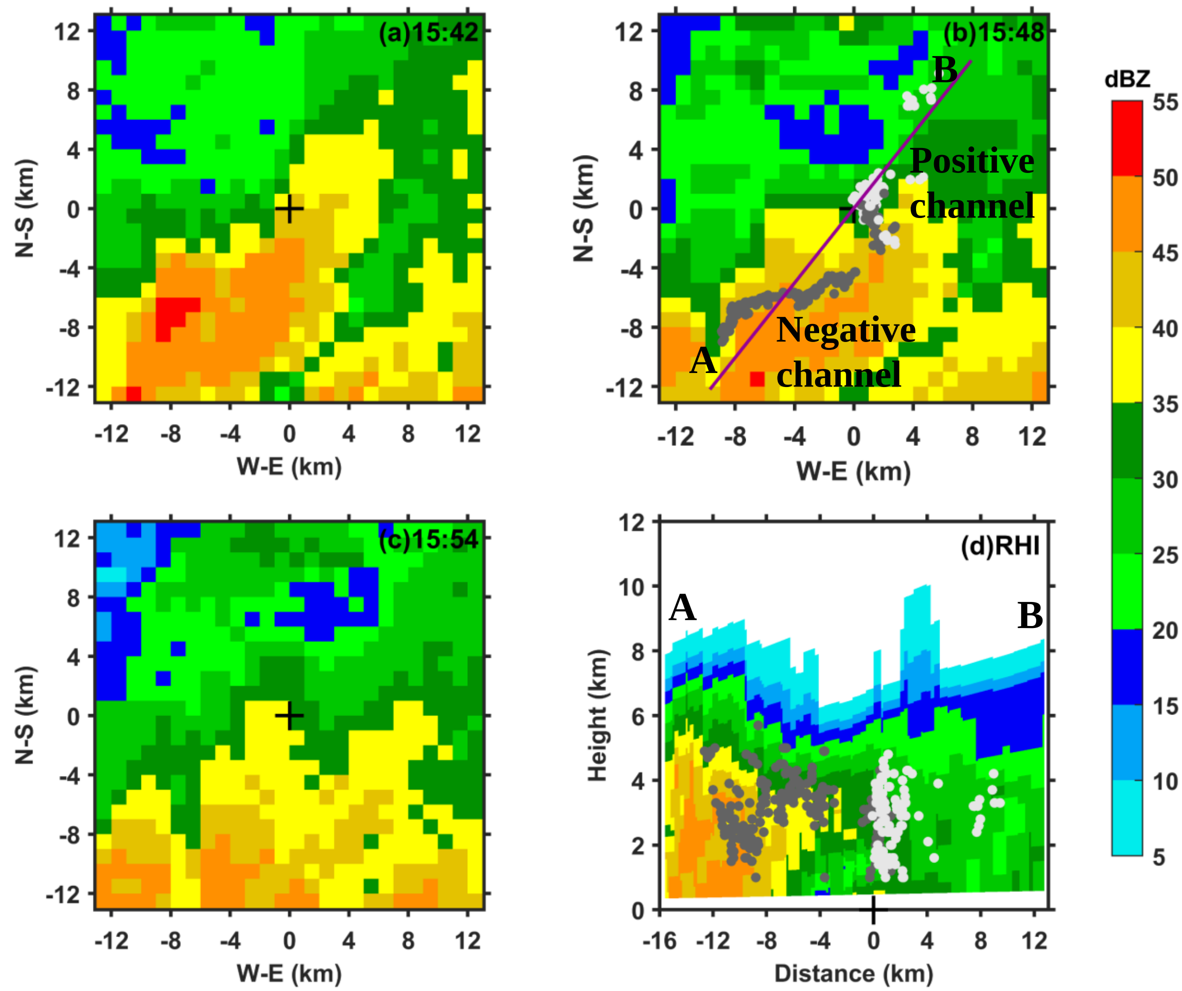
(a)15:42
N-S (km)
W-E (km)
(b)15:48
B
A
Positive channel
Negative channel
(c)15:54
(d)RHI
Height (km)
Distance (km)
dBZ
55
50
45
40
35
30
25
20
15
10
5

649

650

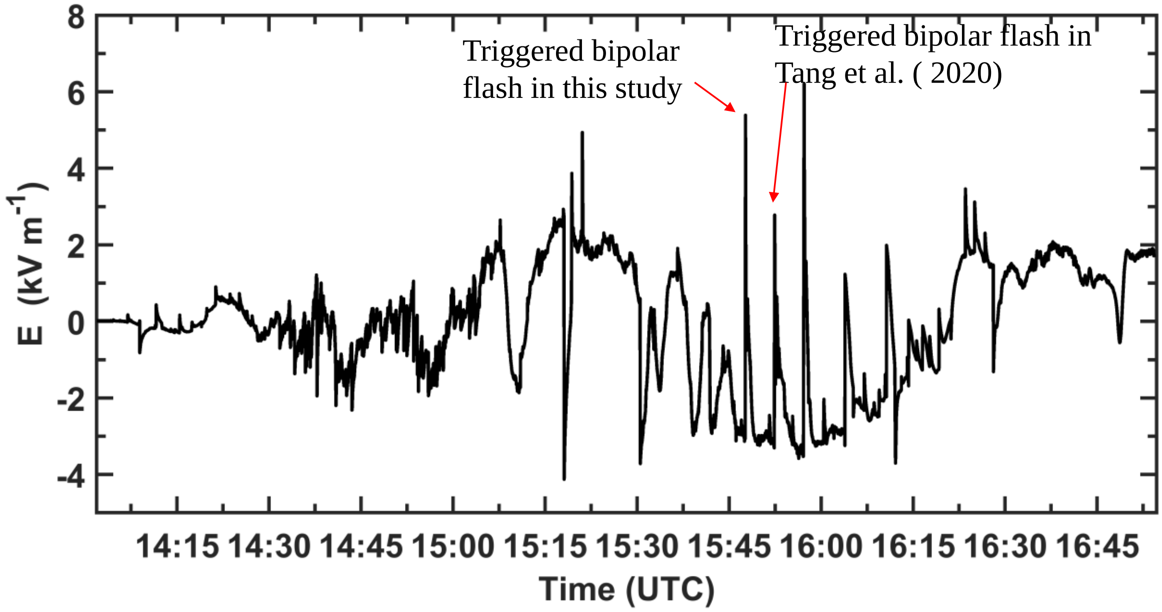
Triggered bipolar
flash in this study
Triggered bipolar flash in
Tang et al. (2020)
8
6
4
2
0
-2
-4
E (kV m-1)
14:15 14:30 14:45 15:00 15:15 15:30 15:45 16:00 16:15 16:30 16:45
Time (UTC)

651

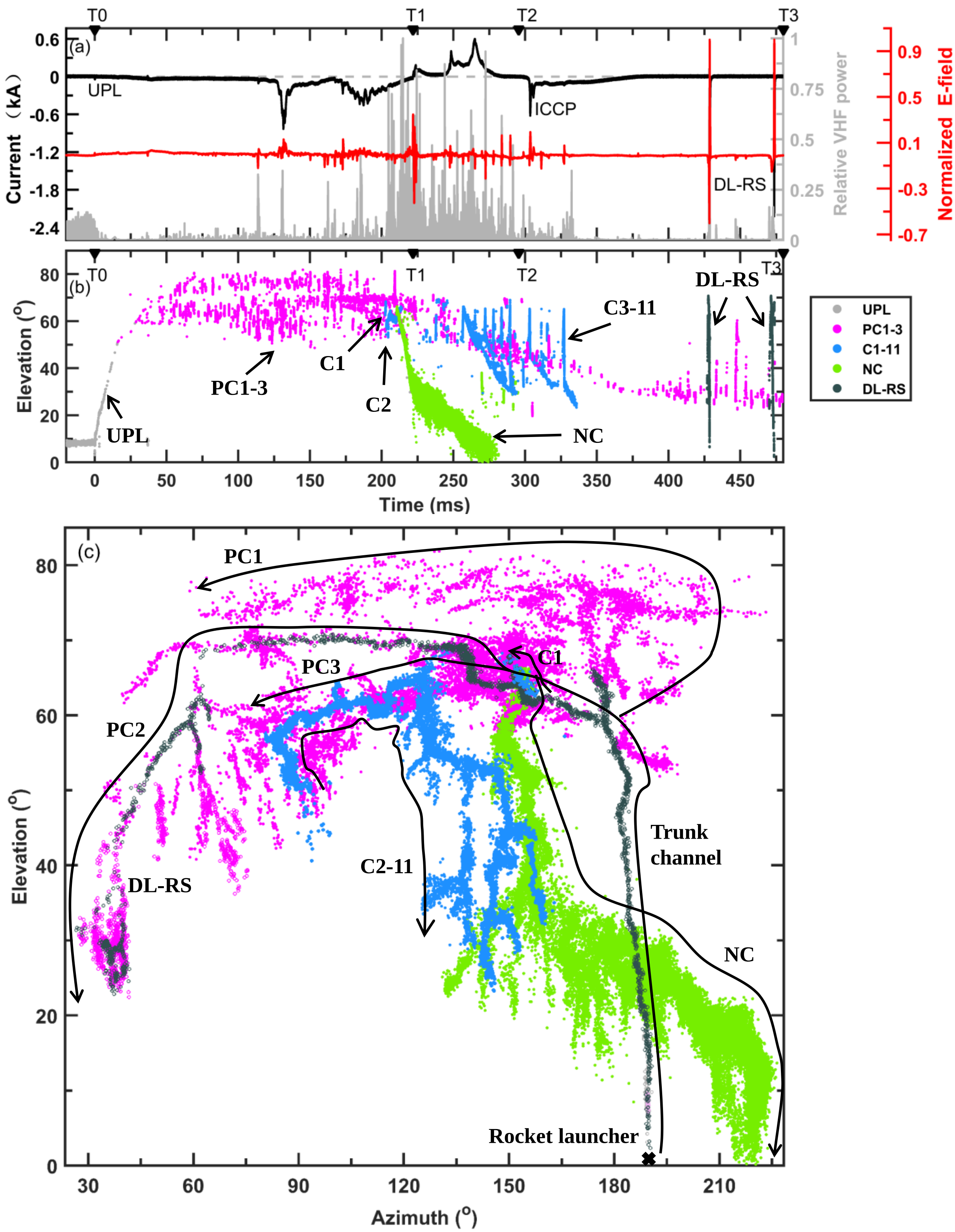

T0
T1
T2
T3
(a)
UPL
ICCP
DL-RS
Current （kA）
Relative VHF power
Normalized E-field
(b)
Elevation (°)
PC1-3
C1
C2
C3-11
NC
DL-RS
UPL
Time (ms)
C1-11
(c)
PC1
PC2
PC3
C1
C2-11
DL-RS
Trunk channel
NC
Rocket launcher
Elevation (°)
Azimuth (°)

652

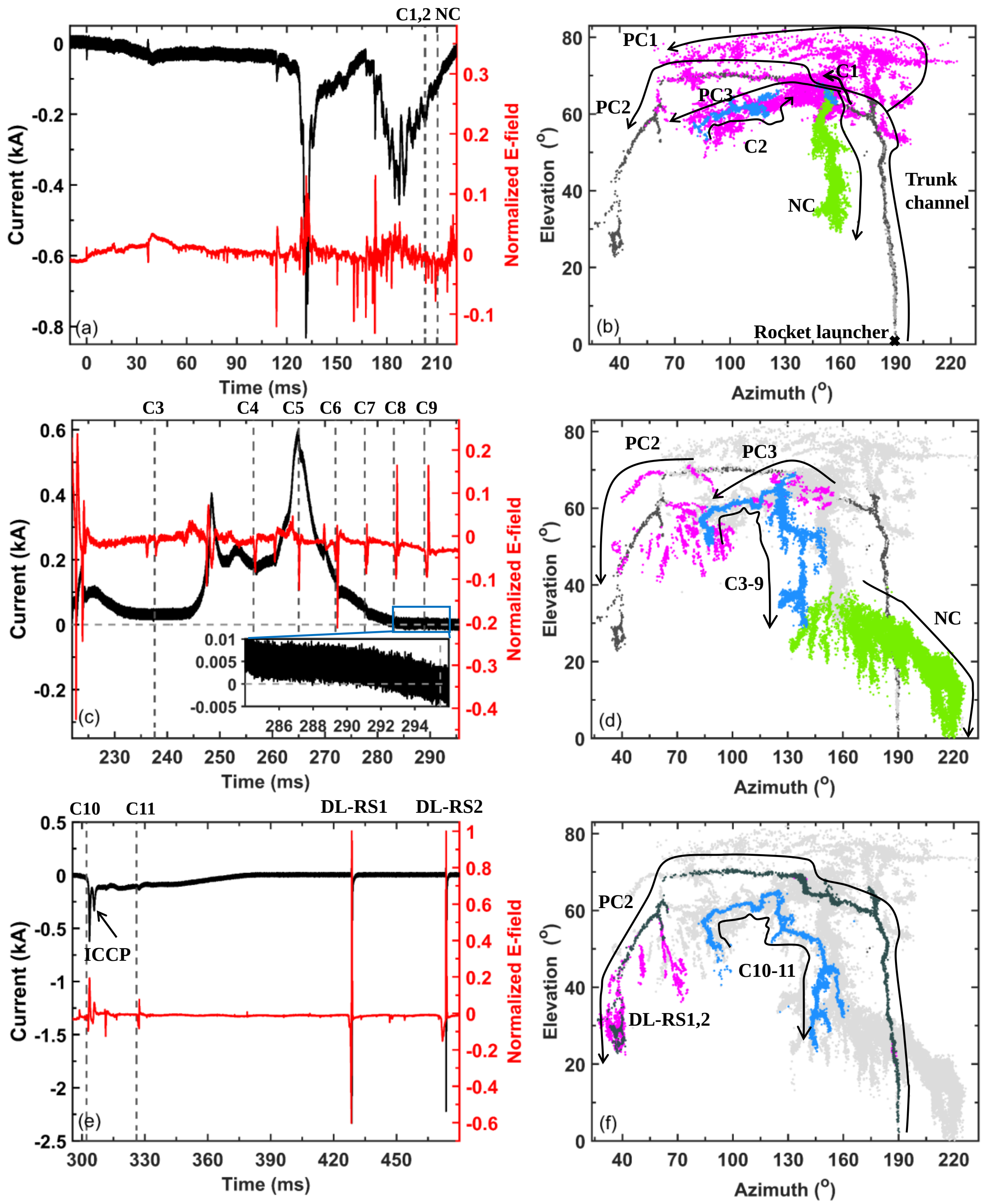
C1,2 NC
Current (kA)
Normalized E-field
Time (ms)
(a)
PC1
C1
PC3
PC2
C2
NC
Trunk channel
Rocket launcher
Elevation (°)
Azimuth (°)
(b)
C3
C4
C5
C6
C7
C8
C9
(c)
PC2
PC3
C3-9
NC
(d)
C10
C11
DL-RS1
DL-RS2
ICCP
(e)
PC2
C10-11
DL-RS1,2
(f)

653

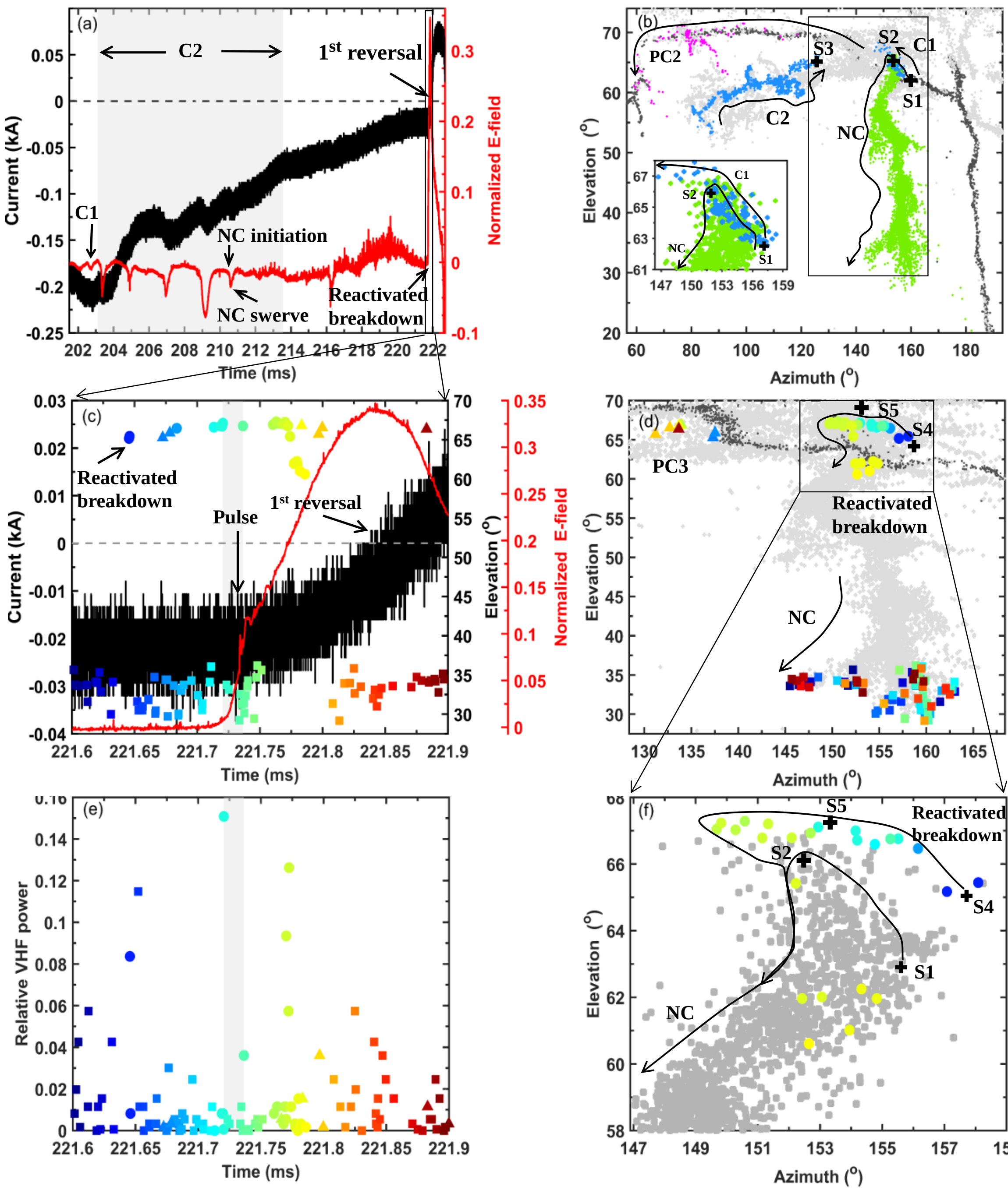

(a)
C2
1st reversal
C1
NC initiation
NC swerve
Reactivated breakdown
Current (kA)
Normalized E-field
Time (ms)
(b)
PC2
S3
S2
C1
S1
C2
NC
Elevation (°)
Azimuth (°)
(c)
Reactivated breakdown
Pulse
1st reversal
Current (kA)
Elevation (°)
Normalized E-field
Time (ms)
(d)
PC3
S5
S4
Reactivated breakdown
NC
ms
Elevation (°)
Azimuth (°)
(e)
Relative VHF power
Time (ms)
(f)
S5
Reactivated breakdown
S2
S4
S1
NC
Elevation (°)
Azimuth (°)

654

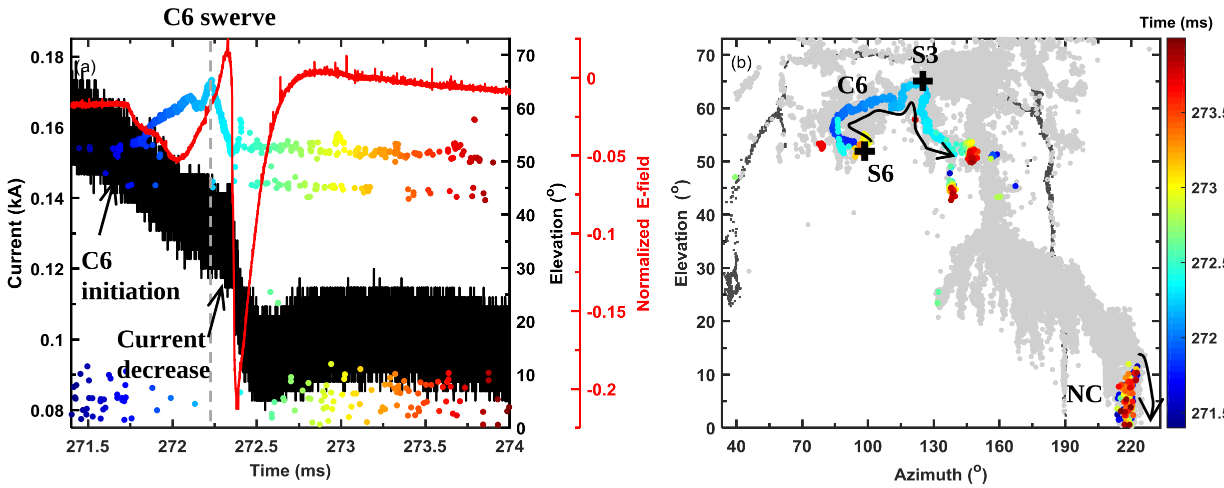
C6 swerve
(a)
C6
initiation
Current
decrease
Current (kA)
Elevation (°)
Normalized E-field
Time (ms)
(b)
S3
C6
S6
NC
Elevation (°)
Azimuth (°)
Time (ms)

655

656

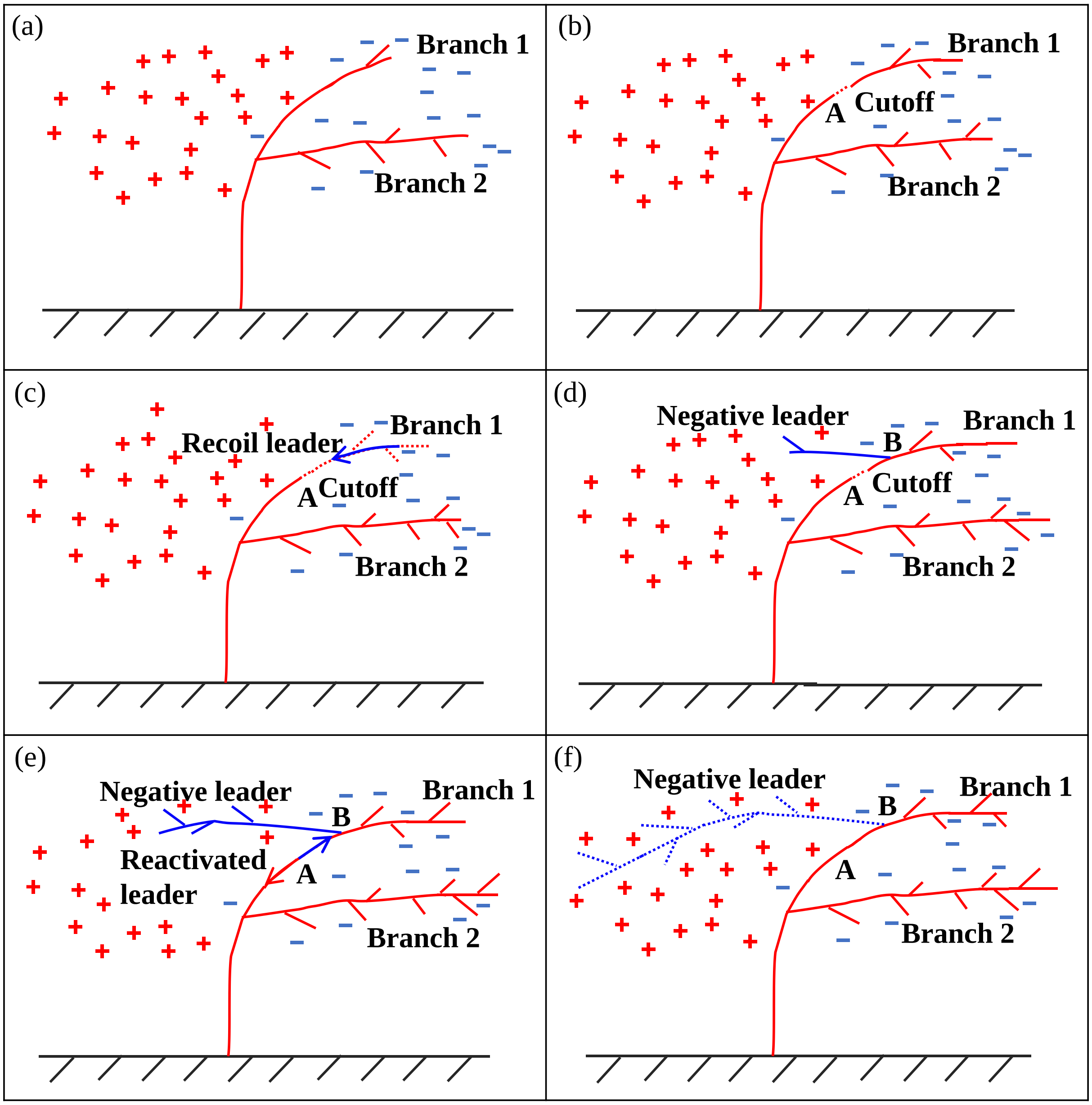
(a)
Branch 1
Branch 2
(b)
Branch 1
A
Cutoff
Branch 2
(c)
Branch 1
Recoil leader
A
Cutoff
Branch 2
(d)
Negative leader
B
Branch 1
A
Cutoff
Branch 2
(e)
Negative leader
B
Branch 1
Reactivated
leader
A
Branch 2
(f)
Negative leader
B
Branch 1
A
Branch 2